Supplementary Information for Planar Tetracoordinate Carbon with Triple C≡C Bonding in C_2Li_3H and $C_2Li_4H_2$ Clusters

Guang-ren Na,[a#] Chagan Dari,[a#] Li-juan Cui,[a] and Zhong-hua Cui*[a,b]

[a]*Institute of Atomic and Molecular Physics, Jilin University, Changchun 130023, China*
[b]*State Key Laboratory of Inorganic Synthesis and Preparative Chemistry, Jilin University, Changchun 130023, China*

**E-mail: zcui@jlu.edu.cn*

#These authors contributed equally to this work.

Section 1. Computational details

The potential energy surfaces of C_2Li_3H and $C_2Li_4H_2$ were explored in both singlet and triplet spin states using the Genetic Algorithm and Structure-driven Approaches (GASA) program. [1] All low-lying candidate structures were fully optimized at the PBE0[2]/aug-cc-pVTZ[3, 4] level with Grimme's D3 dispersion correction[5-7] using the original zero-damping function, and harmonic frequencies at the same level verified each structure as a genuine minimum. Relative energies were refined by single-point CCSD(T) [8]/aug-cc-pVTZ calculations on the PBE0-D3/aug-cc-pVTZ optimized geometries, with zero-point energy corrections taken from the PBE0-D3 frequencies. The PBE0 hybrid functional was chosen for its demonstrated reliability in describing alkali-metal-stabilized planar hypercoordinate carbon clusters. [9-11] T_1 diagnostic[12] values of the converged CCSD wavefunctions for all singlet low-lying isomers (0.015–0.028), including the ptC global minima **1a** and **1b**, support the suitability of single-reference methods; the triplet structures give somewhat larger values (0.027–0.078) but lie at least 37.6 kcal mol^{-1} above the singlet global minima and do not affect the conclusions. The global-minimum ptC minima **1a** and **1b** were further reoptimized at the CCSD(T)/aug-cc-pVTZ level (Fig. S1), yielding geometries in close agreement with the PBE0-D3 ones.

To assess the robustness of the predicted ptC global minima with respect to functional choice, the two lowest-lying isomers of each system (**1a**/**2a** and **1b**/**2b**) were fully reoptimized, with frequency analysis at the B3LYP-D3[13]/aug-cc-pVTZ and ωB97X-D[14]/aug-cc-pVTZ levels. As summarized in Table S3, the ptC structures **1a** and **1b** remain the lowest-energy isomers within each pair across all three DFT functionals as well as at the CCSD(T) reference. Wavefunction stability tests (Stable=Opt in Gaussian 16) were carried out on **1a**, **2a**, **1b** and **2b** at all three DFT levels (aug-cc-pVTZ) confirm that the closed-shell singlet wavefunctions are stable solutions, [15] providing additional reliability to the present DFT results.

Chemical bonding was analyzed at the PBE0-D3/aug-cc-pVTZ level. Wiberg bond indices (WBI) [16] and natural population analysis (NPA) charges[17] were obtained from natural bond orbital (NBO) analysis. Adaptive natural density partitioning (AdNDP)

analysis[18] was performed using the Multiwfn program. [19, 20] Two-dimensional nucleus-independent chemical shift (NICS) [21, 22] maps were computed at the PBE0-D3/aug-cc-pVTZ level using the gauge-including atomic orbital (GIAO) method. Energy decomposition analysis combined with natural orbitals for chemical valence (EDA-NOCV) [23, 24] and interacting quantum atoms (IQA) [25] analyses were performed with the ADF 2023 program[26] at the PBE0-D3/TZ2P-ZORA and PBE0/TZ2P levels, respectively, on the PBE0-D3/aug-cc-pVTZ geometries. The IQA interatomic interaction energy $V_{\mathrm{int}}^{\mathrm{IQA}}$ was decomposed into a classical Coulombic component V^{C} and an exchange–correlation component V^{XC}.

Born–Oppenheimer molecular dynamics (BOMD) [27] simulations were performed at the PBE0-D3/aug-cc-pVTZ level for 20 ps with a 0.5 fs time step at 300 K and 400 K. The vertical detachment energy and excited-state gap of C_2Li_3H were estimated via Koopmans' theorem[28] from the PBE0-D3/aug-cc-pVTZ orbital energies. All electronic-structure calculations except EDA-NOCV and IQA were performed with Gaussian 16, Revision C.01. [29]

NHC-coordinated complexes of C_2Li_3H and $C_2Li_4H_2$ were investigated to assess whether the ptC motif persists in a representative ligand environment. The NHC employed is 1,3-dimethylimidazol-2-ylidene. Candidate coordination modes were constructed by binding NHC to each chemically distinct coordination site of the parent ptC cluster, followed by full geometry optimization and harmonic frequency analysis at the PBE0-D3/aug-cc-pVTZ level. All NHC-bound minima reported are true minima (no imaginary frequencies); relative energies include zero-point corrections at the same level. Optimized structures and relative energies are shown in Fig. S4.

Section 2. Supplementary figures and tables

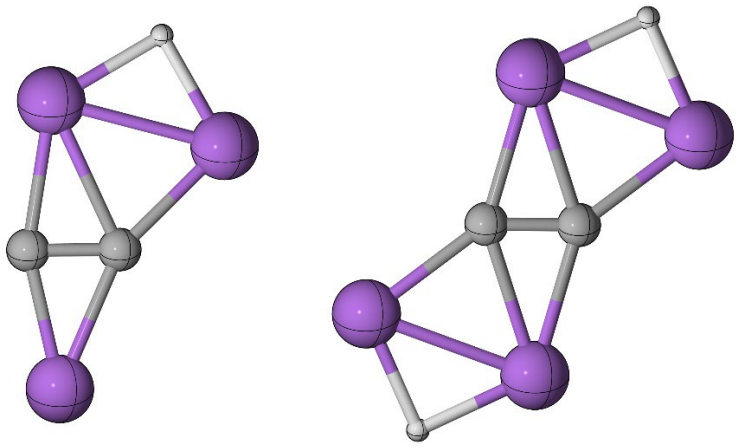

Figure S1. CCSD(T)/aug-cc-pVTZ optimized structures of C_2Li_3H and $C_2Li_4H_2$, confirming ptC geometries as genuine minima.

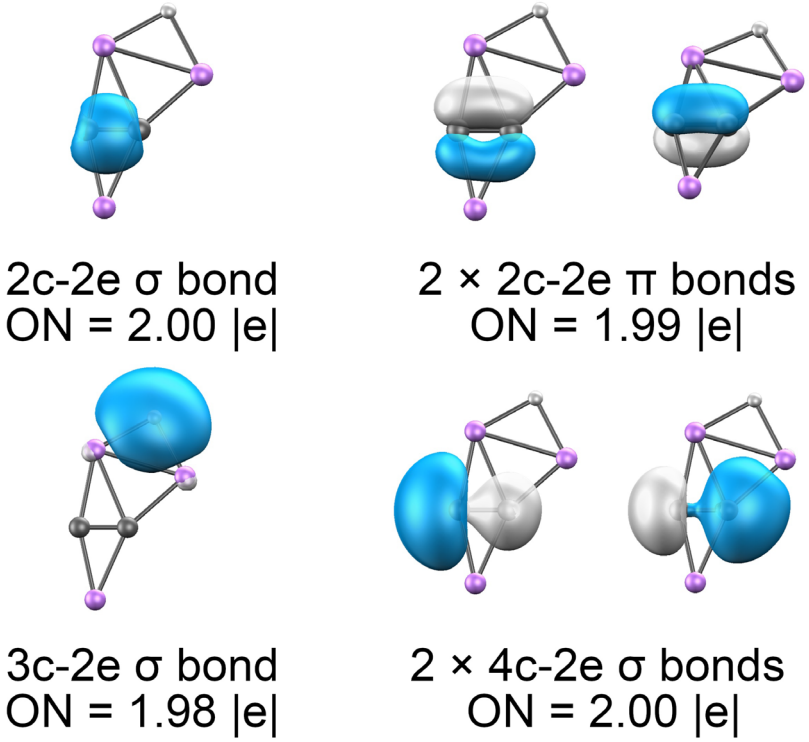

Figure S2. AdNDP analysis of C_2Li_3H at the PBE0-D3/aug-cc-pVTZ level. Occupation numbers (ON) in |e|.

Deformation density	Orbital	C_2^{2-}	$Li_4H_2^{2+}$

$\Delta\rho_{(1)}$	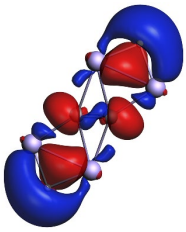 $\Delta E_{orb(1)}$ = -18.9 kcal/mol $\lvert\nu_1\rvert$ = 0.39	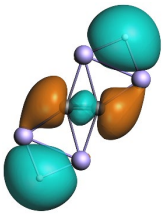 HOMO-1	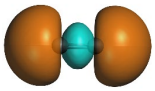 HOMO ν = -0.16	→	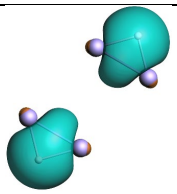 HOMO-1 ν = -0.22 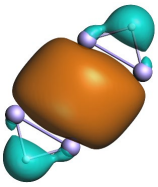 LUMO ν = 0.32
$\Delta\rho_{(2)}$	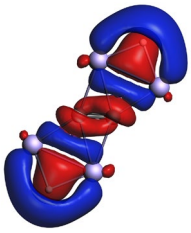 $\Delta E_{orb(2)}$ = -18.1 kcal/mol $\lvert\nu_2\rvert$ = 0.37	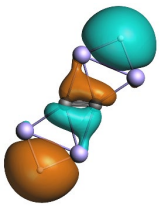 HOMO	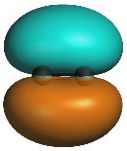 HOMO-1 ν = -0.06	→	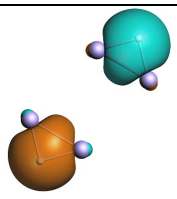 HOMO ν = -0.15 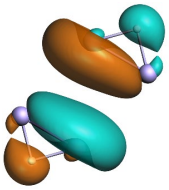 LUMO+3 ν = 0.16
$\Delta\rho_{(3)}$	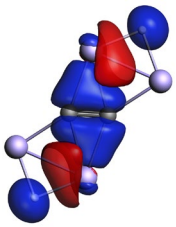 $\Delta E_{orb(3)}$ = -8.5 kcal/mol $\lvert\nu_3\rvert$ = 0.22	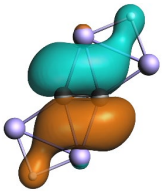 HOMO-4	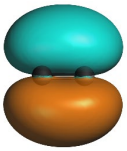 HOMO-1 ν = -0.05	→	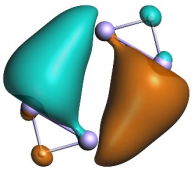 LUMO+1 ν = 0.03
$\Delta\rho_{(4)}$	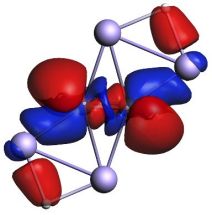 $\Delta E_{orb(4)}$ = -7.9 kcal/mol $\lvert\nu_4\rvert$ = 0.19	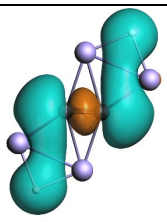 HOMO-3	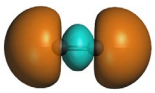 HOMO ν = -0.20	→	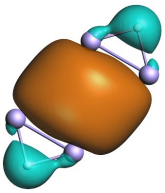 LUMO ν = 0.10

$\Delta\rho_{(5)}$	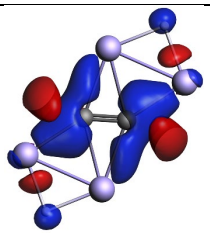	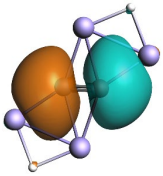	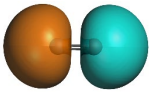	→	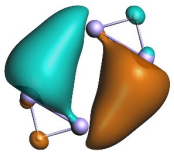
	$\Delta E_{orb(5)}$ = -6.9 kcal/mol $\lvert\nu_5\rvert$ = 0.20	HOMO-5	HOMO-2 ν = -0.15		LUMO+1 ν = 0.09
$\Delta\rho_{(6)}$	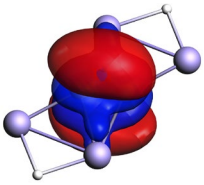	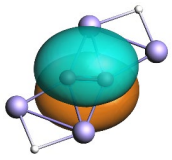	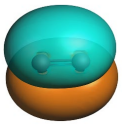	→	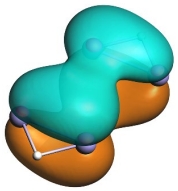
	$\Delta E_{orb(6)}$ = -5.5 kcal/mol $\lvert\nu_6\rvert$ = 0.17	HOMO-2	HOMO-1′ ν = -0.07		LUMO+2 ν = 0.10

Figure S3. Deformation densities ($\Delta\rho$) corresponding to ΔE_{orb} and related interacting orbitals in $C_2Li_4H_2$ at the PBE0-D3/TZ2P-ZORA level, using C_2^{2-} (S) and $Li_4H_2^{2+}$ (S) fragments. Eigenvalues ν indicate charge flow magnitude; direction: red → blue.

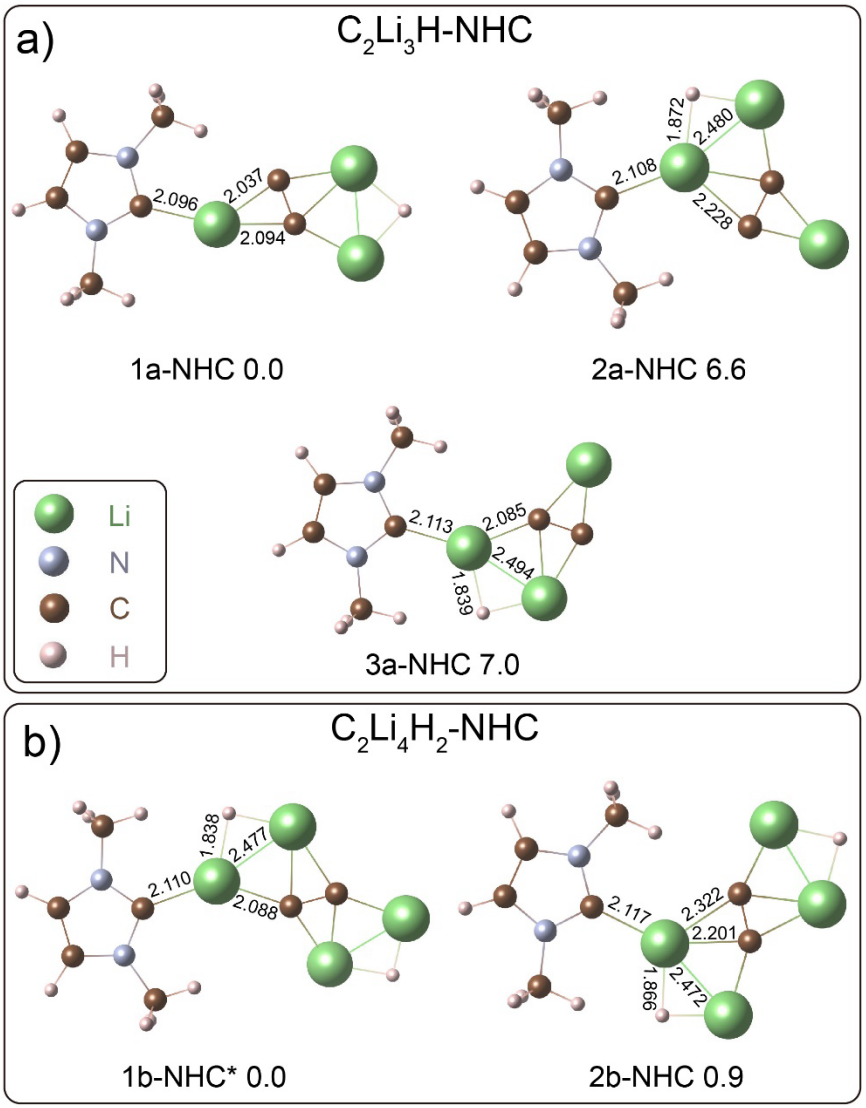

Figure S4. Optimized geometries of NHC-coordinated complexes of (a) C_2Li_3H and (b) $C_2Li_4H_2$ at the PBE0-D3/aug-cc-pVTZ level. Relative energies (kcal mol^{-1}, with zero-point corrections) and Li–C(NHC) bond lengths (Å) are indicated. NHC = 1,3-dimethyl-imidazol-2-ylidene. An asterisk (*) denotes a non-planar isomer in which the Li–H–Li framework twists out of the C≡C plane and the ptC motif is lost.

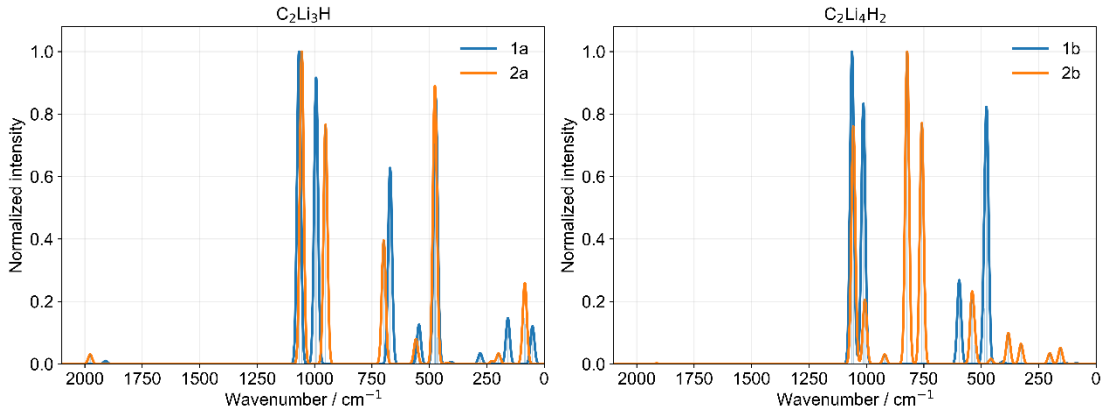

Figure S5. Harmonic IR spectra of the two lowest-lying isomers of (left) C_2Li_3H and (right) $C_2Li_4H_2$ computed at the PBE0-D3/aug-cc-pVTZ level. Blue traces: global-minimum ptC structures (1a and 1b); orange traces: second-lowest isomers (2a and 2b).

Table S1. Electronic energies including zero-point energy (ZPE) corrections for the global minima (**1a**, **1b**) and second-lowest isomers (**2a**, **2b**) of C_2Li_3H and $C_2Li_4H_2$ at different theoretical levels. All structures were fully reoptimized with frequency analysis at each DFT level using the aug-cc-pVTZ basis set; CCSD(T)/aug-cc-pVTZ single-point energies were computed on the PBE0-D3/aug-cc-pVTZ geometries with PBE0-D3/aug-cc-pVTZ ZPE corrections. Absolute energies are reported in Hartree; relative energies ΔE (in kcal mol^{-1}) are taken with respect to the corresponding global minimum within each system.

Method	C_2Li_3H			$C_2Li_4H_2$		
	1a	2a	ΔE	1b	2b	ΔE
PBE0-D3	-99.196	-99.191	3.1	-107.329	-107.321	5.0
CCSD(T)	-99.040	-99.035	3.2	-107.141	-107.134	4.6
B3LYP-D3	-99.387	-99.382	2.6	-107.553	-107.540	8.0
wB97X-D	-99.344	-99.340	2.5	-107.506	-107.503	1.8

Table S2. EDA results of $C_2Li_4H_2$ considering C_2 and Li_4H_2 in different charge and electronic states as interacting fragments at the PBE0-D3/TZ2P-ZORA level. Energy values are given in kcal/mol.

	C_2^{2-} (S) + $Li_4H_2^{2+}$ (S)	C_2^{-} (D) + $Li_4H_2^{+}$ (D)	C_2 (S) + Li_4H_2 (S)

ΔE_{int}	-610.9	-257.6	-242.6
ΔE_{Pauli}	133.3	224.9	265.3
ΔE_{disp}	-0.4	-0.4	-0.4
ΔE_{elstat}	-675.9	-339.4	-226.4
ΔE_{orb}	-67.9	-142.7	-281.1

Table S3. IQA decomposition of selected interatomic interactions in C_2Li_3H at the PBE0/TZ2P level. C5 is the planar tetracoordinate carbon center (coordinated by Li1, Li2, Li3, and C4); V^C is the classical Coulombic term and V^{XC} the exchange–correlation term. Energies in kcal mol^{-1}. Percentages in parentheses give V^{XC}/V_{int}^{IQA}.

Pair	V_{int}^{IQA}	V^C	V^{XC}
ptC coordination environment (C5)			
C5-Li1	-139.8	-128.9	-11.0 (7.8%)
C5-Li2	-174.2	-158.0	-16.2 (9.3%)
C5-Li3	-126.1	-118.6	-7.4 (5.9%)
C5-C4	-316.7	+136.1	-452.8
C4 (non-ptC carbon)			
C4-Li1	-128.1	-112.7	-15.4 (12.0%)
C4-Li2	-56.4	-55.4	-1.0 (1.7%)
C4-Li3	-109.8	-99.1	-10.6 (9.7%)
Peripheral 3c–2e Li–H–Li			
Li2–H6	-152.5	-137.0	-15.6 (10.2%)
Li3–H6	-149.9	-135.3	-14.6 (9.7%)

Table S4. Comparison of C-M exchange-correlation contributions (V^{XC}/V_{int}^{IQA}) from IQA analysis across representative alkali- and alkaline-earth-metal-decorated planar hypercoordinate carbon (and ppCl reference) clusters reported in the literature, together with the present work.

Cluster	C-M pair	V^{XC}/V_{int}^{IQA}	Classification
$CO_3Na_3^+$	C-Na	repulsive	rejected as phC[9]
$CS_3Na_3^+$	C-Na	1.4%	phC[9]

$CSe_3Na_3^+$	C-Na	1.1%	phC[9]
$Li_3CS_2^+$	C–Li	7.7%	ppC[9]
Li_2CS_2	C–Li	11.6%	ppC[9]
Li_2C_5	C–Li	6.4%	phC[30]
Na_2C_5	C-Na	6.8%	phC[30]
K_2C_5	C-K	9.1%	phC[30]
$Be_2C_5^+$	C-Be	3.2%	phC[30]
$Ca_2C_5^+$	C-Be	9.1%	phC[30]
Al_2C_5	C-Al	7.6%	phC[30]
$Cl@Li_5Cl_5^-$	Cl–Li	4.7%	ppCl[31]
$C_2Li_4H_2$ (this work)	C–Li	6.9–9.8%	ptC

Cartesian coordinates (PBE0-D3/aug-cc-pVTZ)

1a

Li	-1.935491	1.195225	0.000000
Li	1.998098	0.607997	0.000000
Li	0.849143	-1.554339	0.000000
C	-0.878844	-0.422081	0.000000
C	0.000000	0.471975	0.000000
H	2.537816	-1.046014	0.000000

2a

H	-2.826435	-0.163340	0.000000
Li	2.532577	-0.991380	0.000000
C	0.779122	-0.306943	0.000000
Li	-1.266575	-0.997924	0.000000
Li	-1.882101	1.322325	0.000000
C	0.000000	0.667656	0.000000

3a

H	2.044715	-0.338775	0.000000
Li	0.785863	0.563944	1.203811

C	-0.707001	-0.448982	0.000000
Li	0.785863	0.563944	-1.203811
Li	0.785863	-1.715187	0.000000
C	-0.812579	0.799094	0.000000
4a			
C	0.000000	0.818416	0.000000
Li	1.827721	-3.085808	0.000000
H	-2.210670	1.426177	0.000000
Li	-0.511980	-1.173379	0.000000
Li	1.811002	-0.041508	0.000000
C	-1.194926	1.094235	0.000000
5a			
C	0.546535	-1.101372	0.000000
C	-0.426684	-0.349399	0.000000
Li	-1.790432	1.183764	0.000000
Li	0.546535	1.155461	1.337786
H	1.372974	-1.779427	0.000000
Li	0.546535	1.155461	-1.337786
6a			
C	0.000000	0.000000	-0.100218
Li	0.000000	2.068657	-0.331752
C	0.000000	0.000000	1.134301
Li	0.000000	-2.068657	-0.331752
H	0.000000	0.000000	2.203575
Li	0.000000	0.000000	-2.139187
7a			
Li	-0.720094	-1.282124	0.000000
H	-2.205541	1.306931	0.000000
Li	1.965242	0.243950	0.000000
Li	1.872592	-2.697656	0.000000

C	0.000000	0.680361	0.000000
C	-1.191280	0.969732	0.000000

8a

C	0.667553	-0.779099	0.000000
C	-0.531566	-0.357790	0.000000
H	1.277773	-1.673073	0.000000
Li	-2.033004	0.861361	0.000000
Li	0.667553	0.985054	1.212406
Li	0.667553	0.985054	-1.212406

1b

Li	-1.178559	1.664921	-0.000000
Li	-1.178559	-2.253810	0.000000
Li	1.178559	-1.664921	-0.000000
C	0.514141	0.355328	-0.000000
C	-0.514141	-0.355328	-0.000000
H	0.295561	-3.176267	0.000000
Li	1.178559	2.253810	0.000000
H	-0.295561	3.176267	0.000000

2b

Li	-1.862096	0.000000	-0.099448
Li	1.862096	0.000000	-0.099448
Li	0.000000	1.141225	1.223207
Li	0.000000	-1.141225	1.223207
C	0.000000	-0.625989	-0.838403
C	0.000000	0.625989	-0.838403
H	1.436809	0.000000	1.659140
H	-1.436809	0.000000	1.659140

3b

Li	0.000000	2.274510	0.167454
Li	0.000000	-2.274510	0.167454

Li	1.063894	0.000000	1.016534
Li	-1.063894	0.000000	1.016534
C	0.000000	0.625515	-0.880543
C	0.000000	-0.625515	-0.880543
H	0.000000	-1.418878	1.731295
H	0.000000	1.418878	1.731295

4b

Li	1.643320	-2.611660	0.000000
Li	-1.051610	2.542551	0.000000
Li	-0.933660	-1.372960	0.000000
Li	1.919163	0.127014	0.000000
C	0.000000	0.720808	0.000000
C	-1.248795	0.635619	0.000000
H	-0.040508	-2.847025	0.000000
H	2.801640	-1.346372	0.000000

5b

Li	0.000000	0.000000	-1.847578
Li	0.000000	0.000000	2.442391
Li	0.000000	2.252757	-0.633933
Li	0.000000	-2.252757	-0.633933
C	0.000000	-0.624856	0.543099
C	0.000000	0.624856	0.543099
H	0.000000	1.757942	-2.249017
H	0.000000	-1.757942	-2.249017

6b

Li	-3.050686	1.085989	0.000000
Li	2.433140	-2.006460	0.000000
Li	1.997229	0.711901	0.000000
Li	-0.274809	-1.350503	0.000000
C	0.000000	0.735672	0.000000

C	-1.234484	0.570637	0.000000
H	3.239154	-0.494337	0.000000
H	0.853128	-2.666299	0.000000

7b

Li	2.008069	-0.670239	0.000000
Li	-1.255397	2.076976	0.000000
Li	0.073646	-0.885397	1.604222
Li	0.073646	-0.885397	-1.604222
C	0.073646	0.553235	0.000000
C	-1.090877	0.082959	0.000000
H	1.701747	-1.362498	1.637079
H	1.701747	-1.362498	-1.637079

8b

Li	-1.935368	0.616949	0.000000
Li	-1.825576	-2.236650	0.000000
Li	0.087714	-0.834821	1.296931
Li	0.087714	-0.834821	-1.296931
C	0.087714	0.900856	0.000000
C	1.317140	0.923459	0.000000
H	2.380580	1.034318	0.000000
H	-0.053152	-2.112181	0.000000

References

(1) Liu, X.-b.; Cui, Z.-h. Genetic Algorithm and Structure-driven Approaches for atomic clusters (GASA). *Jilin University* **2024**.

(2) Adamo, C.; Barone, V. Toward reliable density functional methods without adjustable parameters: The PBE0 model. *The Journal of Chemical Physics* **1999**, *110* (13), 6158-6170.

(3) Kendall, R. A.; Dunning, T. H., Jr.; Harrison, R. J. Electron affinities of the first-row atoms revisited. Systematic basis sets and wave functions. *The Journal of Chemical Physics* **1992**, *96* (9), 6796-6806.

(4) Woon, D. E.; Dunning, T. H., Jr. Gaussian basis sets for use in correlated molecular calculations. III. The atoms aluminum through argon. *The Journal of Chemical Physics* **1993**, *98* (2), 1358-1371.

(5) Grimme, S.; Antony, J.; Ehrlich, S.; Krieg, H. A consistent and accurate ab initio parametrization of density functional dispersion correction (DFT-D) for the 94 elements H-Pu. *The Journal of Chemical Physics* **2010**, *132* (15).

(6) Grimme, S.; Ehrlich, S.; Goerigk, L. Effect of the damping function in dispersion corrected density functional theory. *Journal of Computational Chemistry* **2011**, *32* (7), 1456-1465.
(7) Peterson, K. A.; Figgen, D.; Goll, E.; Stoll, H.; Dolg, M. Systematically convergent basis sets with relativistic pseudopotentials. II. Small-core pseudopotentials and correlation consistent basis sets for the post-d group 16–18 elements. *The Journal of Chemical Physics* **2003**, *119* (21), 11113-11123.
(8) Purvis, G. D., III; Bartlett, R. J. A full coupled-cluster singles and doubles model: The inclusion of disconnected triples. *The Journal of Chemical Physics* **1982**, *76* (4), 1910-1918.
(9) Leyva-Parra, L.; Diego, L.; Yañez, O.; Inostroza, D.; Barroso, J.; Vásquez-Espinal, A.; Merino, G.; Tiznado, W. Planar Hexacoordinate Carbons: Half Covalent, Half Ionic. *Angewandte Chemie International Edition* **2021**, *60* (16), 8700-8704.
(10) Leyva-Parra, L.; Diego, L.; Inostroza, D.; Yañez, O.; Pumachagua-Huertas, R.; Barroso, J.; Vásquez-Espinal, A.; Merino, G.; Tiznado, W. Planar Hypercoordinate Carbons in Alkali Metal Decorated CE_3^{2-} and CE_2^{2-} Dianions. *Chemistry – A European Journal* **2021**, *27* (67), 16701-16706.
(11) Guo, J.; Chai, H.; Duan, Q.; Qin, J.; Shen, X.; Jiang, D.; Hou, J.; Yan, B.; Li, Z.; Gu, F.; et al. Planar tetracoordinate carbon species CLi3E with 12-valence-electrons. *Physical Chemistry Chemical Physics* **2016**, *18* (6), 4589-4593.
(12) Lee, T. J.; Taylor, P. R. A diagnostic for determining the quality of single-reference electron correlation methods. *International Journal of Quantum Chemistry* **1989**, *36* (S23), 199-207.
(13) Stephens, P. J.; Devlin, F. J.; Chabalowski, C. F.; Frisch, M. J. Ab Initio Calculation of Vibrational Absorption and Circular Dichroism Spectra Using Density Functional Force Fields. *The Journal of Physical Chemistry* **1994**, *98* (45), 11623-11627.
(14) Chai, J.-D.; Head-Gordon, M. Long-range corrected hybrid density functionals with damped atom–atom dispersion corrections. *Physical Chemistry Chemical Physics* **2008**, *10* (44), 6615-6620.
(15) Bauernschmitt, R.; Ahlrichs, R. Stability analysis for solutions of the closed shell Kohn–Sham equation. *The Journal of Chemical Physics* **1996**, *104* (22), 9047-9052.
(16) Wiberg, K. B. Application of the pople-santry-segal CNDO method to the cyclopropylcarbinyl and cyclobutyl cation and to bicyclobutane. *Tetrahedron* **1968**, *24* (3), 1083-1096.
(17) Reed, A. E.; Weinstock, R. B.; Weinhold, F. Natural population analysis. *The Journal of Chemical Physics* **1985**, *83* (2), 735-746.
(18) Zubarev, D. Y.; Boldyrev, A. I. ”Developing paradigms of chemical bonding: adaptive natural density partitioning. *Physical Chemistry Chemical Physics* **2008**, *10* (34), 5207-5217.
(19) Lu, T.; Chen, F. Multiwfn: A multifunctional wavefunction analyzer. *Journal of Computational Chemistry* **2012**, *33* (5), 580-592.
(20) Lu, T. A comprehensive electron wavefunction analysis toolbox for chemists, Multiwfn. *The Journal of Chemical Physics* **2024**, *161* (8).
(21) Schleyer, P. R. v.; Jiao, H. What is aromaticity? *Pure and Applied Chemistry* **1996**, *68* (2), 209-218.
(22) Schleyer, P. v. R.; Maerker, C.; Dransfeld, A.; Jiao, H.; van Eikema Hommes, N. J. R. Nucleus-Independent Chemical Shifts: A Simple and Efficient Aromaticity Probe. *Journal of the American Chemical Society* **1996**, *118* (26), 6317-6318.
(23) Zhao L, P. S., Frenking G. *in Comprehensive Computational Chemistry*; Elsevier, 2024.
(24) Zhao, L.; von Hopffgarten, M.; Andrada, D. M.; Frenking, G. Energy decomposition analysis. *WIREs Computational Molecular Science* **2018**, *8* (3), e1345.
(25) Blanco, M. A.; Martín Pendás, A.; Francisco, E. Interacting Quantum Atoms: A Correlated Energy Decomposition Scheme Based on the Quantum Theory of Atoms in Molecules. *Journal of Chemical*

Theory and Computation **2005**, *1* (6), 1096-1109.
(26) te Velde, G.; Bickelhaupt, F. M.; Baerends, E. J.; Fonseca Guerra, C.; van Gisbergen, S. J. A.; Snijders, J. G.; Ziegler, T. Chemistry with ADF. *Journal of Computational Chemistry* **2001**, *22* (9), 931-967.
(27) Bakken, V.; Millam, J. M.; Bernhard Schlegel, H. Ab initio classical trajectories on the Born–Oppenheimer surface: Updating methods for Hessian-based integrators. *The Journal of Chemical Physics* **1999**, *111* (19), 8773-8777.
(28) Koopmans, T. Über die Zuordnung von Wellenfunktionen und Eigenwerten zu den Einzelnen Elektronen Eines Atoms. *Physica* **1934**, *1* (1), 104-113.
(29) *Gaussian 16 Rev. C.01*; Wallingford, CT, 2016.
(30) Inostroza, D.; Leyva-Parra, L.; Yañez, O.; Solar-Encinas, J.; Vásquez-Espinal, A.; Valenzuela, M. L.; Tiznado, W. Searching for Systems with Planar Hexacoordinate Carbons. *Atoms* **2023**, *11* (3), 56.
(31) Bai, L.-X.; Gao, C.-Y.; Guo, J.-C.; Li, S.-D. $Cl©Li_5Cl_5^-$: A Star-like Superhalogen Anion Featuring a Planar Pentacoordinate Chlorine at the Center. *Molecules* **2024**, *29* (16), 3831.